Anti-amyloid therapy and cerebral blood flow changes on Magnetic Resonance Imaging: a potential longitudinal biomarker of treatment response?

Andres Ricaurte-Fajardo, Jana Ivanidze, Deborah Zhang, Meem Mahmud, Weiye Yasen , Lisa Ravdin, Silky Pahlajani, Mony de Leon, Anna S. Nordvig[†], Gloria C. Chiang[†]*.

ABSTRACT

Amyloid-targeting therapy has recently become widely available in the U.S. for the treatment of patients with symptomatic mild Alzheimer's disease (AD). At present, there are no biomarkers that have been clinical validated to assess treatment response in routine clinical practice; longitudinal amyloid PET could play a role but is not cost effective. This report presents a case series of six patients with AD, whose amyloid positivity was confirmed by PET or CSF biomarkers, who underwent baseline and longitudinal arterial spin-labeling magnetic resonance imaging (ASL-MR) as part of FDA-mandated, clinical standard-of-care, non-contrast MR monitoring to assess for amyloid-related imaging abnormalities (ARIA). We and others have previously reported that ASL-MR can screen for neurodegenerative disease, as a proxy for FDG-PET, and can be easily added on as a cost-effective, repeatable method to monitor post-therapy changes. This series highlights varied cerebral blood flow (CBF) changes in response to lecanemab therapy. For instance, Cases 1, 3, and 5 showed increased CBF after multiple infusions, with subjective cognitive improvement in Case 1 and improved MoCA scores in Case 3. Case 2 showed improved CBF initially before the 5th infusion, but this returned to baseline on the subsequent study, with no cognitive improvement over the course of therapy. Cases 4 and 6 have demonstrated no significant changes in regional CBF thus far on therapy, with cognitive decline in Case 4. This case series underscores the potential utility of ASL-MR as an adjunct sequence to current imaging protocols to monitor treatment response to anti-amyloid therapy.

ABBREVIATIONS: ASL-MR= arterial spin-labeling magnetic resonance imaging; **MRI=** magnetic resonance imaging; **CBF=** cerebral blood flow; **AD=** Alzheimer's disease; **PET=** positron emission tomography; **CSF=** cerebrospinal fluid; **FDG=** fluorodeoxyglucose.

Received: November 6th, 2024; accepted after revision: December 30th, 2024.
From the Department of **Department of Radiology, Brain Health Imaging Institute (A.R-F, J.I, S.P, M.d,** G.C.C) **Weill Cornell Medicine, New York-Presbyterian Hospital, New York, New York, USA; the Department of Neurology (A.R-F), Pontificia Universidad Javeriana, Bogota, Colombia; the Department of Radiology, Division of Molecular Imaging and Therapeutics (A.R-F, J.I) Weill Cornell Medicine, New York-Presbyterian Hospital, New York, New York, USA; the Department of Neurology (D.Z, MM, L.R, A.S.N) Weill Cornell Medicine, New York-Presbyterian Hospital, New York, New York, USA**

[†]ASN and GCC contributed equally to this manuscript.

Disclosures:

Andres Ricaurte-Fajardo has received compensation as speaker for Siemens Healthineers (unrelated to this manuscript).

Jana Ivanidze has been the recipient of research funding from Novartis Pharmaceuticals, General Electric Healthcare, and Curium Pharma (unrelated to this manuscript; funds paid to institution).

Gloria C. Chiang has received consulting fees from Life Molecular Imaging (unrelated to this manuscript) and speaker honoraria from Efficient CME and PeerView (unrelated to this manuscript).

The remaining authors declare no conflicts of interest related to the content of this article.

Grant Support

Research reported in this publication was supported in part by the following grants: National Institutes of Health/National Institute on Aging R01AG068398 (Gloria C. Chiang), R01AG080011 (Gloria C. Chiang), R01 AG085972 (Gloria C. Chiang), R56 AG058913 (Mony de Leon), and RF1 AG057570 (Mony de Leon), Sonia Jaye and Edward Barsukov Foundation (Anna S. Nordvig), Feil II Clinical Scholar Award (Anna S. Nordvig)

Presentation

Two cases were presented in abbreviated form at the AAIC 2024 meeting

INTRODUCTION

For the past year, lecanemab has been increasingly available in the U.S. for the treatment of symptomatic mild cognitive impairment or mild dementia due to Alzheimer's disease (AD) (1), and donanemab was recently approved for the same indication (2). To qualify for therapy, patients have to undergo amyloid positron emission tomography (PET) or cerebrospinal fluid (CSF) assays (1) to confirm presence of amyloid pathology. Lecanemab is a recombinant humanized IgG1 monoclonal antibody that targets amyloid oligomers, protofibrils, and insoluble fibrils (3). It binds preferentially to protofibrils, which are a high molecular weight form of soluble amyloid and are a component of amyloid plaques (3). Despite its availability, at present, there are no biomarkers that have been clinical validated to assess treatment response in routine clinical practice; longitudinal amyloid PET could play a role but is not cost effective. While lecanemab has shown a modest impact on cognition over 18 months, slowing cognitive decline by 27%, there is minimal detectable cognitive impact in the first six months of treatment and very little is known about the brain's response to therapy. Therefore, tracking early medication effects remains elusive for clinicians (4).

The FDA mandates serial non-contrast MRI scans to monitor for amyloid-related imaging abnormalities (ARIA) while receiving bimonthly lecanemab treatment (prior to the 5th, 7th, and 14th infusions) (1). Additionally, an MRI scan at week 52 (before the 26th infusion) is suggested, particularly for apolipoprotein E ε4 carriers, who have increased risk of ARIA, and for those who had ARIA on prior studies (1).

Arterial spin-labeling MRI (ASL-MR) uses magnetically labeled water (i.e. blood) as an endogenous tracer to measure cerebral blood flow (CBF) in the brain (5,6,7). Unlike other perfusion imaging techniques that use ^{15}O-PET or dynamic imaging with gadolinium contrast, ASL-MR does not require an external tracer or ionizing radiation (7). CBF, estimated by ASL-MR, is closely linked to brain metabolism and associates with FDG-PET, thus representing an efficient, low-cost, non-invasive and quantitative method for evaluating brain function (5,6,7).

In this report, we present six cases of patients with AD, whose amyloid positivity was confirmed by PET or CSF biomarkers, who underwent serial ASL-MR while on lecanemab therapy **(Table 1)**. All patients were imaged on the same clinical 3 Tesla GE SIGNA Architect MRI scanner (GE Medical Systems, Milwaukee, WI, USA). The 3D pseudo-continuous ASL-MR clinical product sequence had the following parameters: PLD 2025 ms, TR 4876, TE 53.6, 38 x 4 mm axial slices, FOV 24, matrix size 512; the scanning time was 4 minutes and 24 seconds **(Online Supplemental File)**. CBF maps were processed using the GE AW Server version 3.2 extension 4.0, set to a range of 0-80 mL/100g/min using the rainbow color scheme. Images were visually interpreted in native space. Regions-of-interest were also placed on the CBF maps to assess quantitative changes over the course of therapy **(Figure 1, Online Supplemental File).** All patients had well-controlled, stable comorbidities, and all followed treatment guidelines for initiation of therapy and monitoring. All cases were followed clinically up to the time of the writing of this manuscript, which was at least to the 14th infusion for Cases 1, 3, 4. We hypothesized that anti-amyloid therapy would lead to improved cerebral perfusion as seen on ASL-MR, potentially due to clearance of both parenchymal and vascular amyloid (8). Here, we present the CBF maps of these patients at baseline and while receiving lecanemab, illustrating the potential utility of ASL-MR in monitoring the effects of lecanemab on brain perfusion.

Case Series

Case 1:

A 77-year-old right-handed woman with a medical history of hyperlipidemia, hypertension and heart failure, with an APOE ε3/ε3 genotype, presented with a 1.5-year history of progressive short-term memory loss, word-finding difficulty, occasional disorientation, and computer apraxia. Symptoms possibly began after parotid gland surgery, during which she experienced mild postoperative delirium. Her baseline Montreal Cognitive Assessment (MoCA) score was 23 out of 30. FDG-PET showed symmetric temporoparietal hypometabolism, a typical pattern for AD **(Online Supplemental File)**, and ASL-MR revealed decreased CBF in the left parietal and temporal lobes, as well as the bilateral frontal lobes **(Figure 2)**. A positive amyloid PET confirmed the diagnosis of AD **(Online Supplemental File)**. She started treatment with lecanemab, and ASL-MR performed at the time of the monitoring MRI scans, before the 5th, 7th, and 14th infusions, showed no ARIA and markedly improved CBF compared to baseline, most notably before the 14th infusion **(Figure 2)**. The patient and family reported subjective cognitive improvement, although the MOCA score remained unchanged at 23/30 after 6 months of therapy. Notably, there was no change in mild volume loss or minimal burden of white matter hyperintensities over the course of therapy **(Online Supplemental File).**

Case 2:

A 59-year-old right-handed woman presented with an 8-month history of progressive short-term memory loss, confusion, and increased anxiety. She struggled with tasks such as understanding the calendar and organizing simple work assignments. The patient had normal walking, with no shuffling or dragging of feet, and reported no urinary incontinence. Her initial MoCA score was 20/30; her APOE genotype was ε3/ε3. FDG-PET showed temporoparietal hypometabolism, and MRI showed marked volume loss and decreased CBF in the bilateral temporal and parietal lobes, as well as the frontal lobes **(Figure 3, Online Supplemental File)**. CSF analysis confirmed the diagnosis of early-onset AD. She began treatment with donepezil, followed by lecanemab. The patient reported feeling less anxious and more socially active, although cognitive challenges persisted. The CBF map showed marked improvement on the scan before the 5th infusion, but the CBF then decreased on the subsequent scan before the 7th dose **(Figure 3)**. There was no evidence of ARIA; the minimal burden of white matter hyperintensities stayed stable **(Online Supplemental File)**.

Case 3:

A 74-year-old right-handed man presented with a 10-year history of slowly progressive memory decline, as well as lifelong depression, monoclonal gammopathy of unknown significance with paresthesias, prostate cancer, and sleep apnea. Three paternal relatives were reported to have a history of cognitive impairment. His baseline MoCA score was 22/30 with deficits in executive function, visuospatial tasks, and short-term recall; his APOE genotype was ε3/ε3. Baseline FDG-PET showed frontal hypometabolism initially favored to represent mild frontotemporal dementia, while MRI showed mild global volume loss and decreased CBF in the bilateral parietal, temporal, and frontal lobes **(Figure 4, Online Supplemental File)**. CSF biomarkers were indeterminate, but subsequent amyloid and tau PET scans were positive, confirming AD **(Online Supplemental File)**. Monitoring MRI scans before the 5th, 7th, and 14th lecanemab infusions showed no evidence of ARIA and continued improvement in CBF **(Figure 4),** despite no change in mild volume loss and minimal burden of white matter hyperintensities **(Online Supplemental File)**. The patient reported improved working memory and overall cognitive function; the pre-lecanemab MoCA score on donepezil (26/30) improved after 6 months of lecanemab therapy to 29/30.

Case 4:

A 62-year-old right-handed man presented with progressive cognitive decline over 2.5 years and worsened anxiety after a suspected COVID infection. His medical history included hypertension and concussion. Cognitive assessments revealed deficits in visuospatial organization, working memory, attention, and orientation. Neuropsychological testing indicated performance below expectation, compared to education-based norms, in multiple cognitive domains, with significant deficits in visuoperceptual ability, working memory, and verbal fluency. His APOE genotype was ε3/ε3.

FDG-PET showed temporoparietal hypometabolism, and MRI showed decreased CBF bilaterally in the temporal, parietal, and frontal lobes **(Figure 5)**. CSF biomarkers and amyloid PET confirmed AD with an associated inflammatory profile, including elevated oligoclonal bands, possibly triggered by COVID infection. Donepezil, memantine, and desvenlafaxine somewhat improved symptoms. Five days of high-dose methylprednisolone very briefly improved executive function, mood, and alertness. He had one microhemorrhage at baseline, but he did not develop ARIA. ASL-MR before the 5th, 7th, and 14th dose monitoring scans for lecanemab did not show improvement in CBF compared to baseline **(Figure 5)**. Clinical history indicated slight decrease in cognitive function; the pre-lecanemab MMSE of 22/30 decreased slightly to 21/30 after 9 months of lecanemab therapy. There was no change in mild-moderate volume loss **(Online Supplemental File)**. He had no white matter hyperintensities at baseline or on subsequent MRI scans.

Case 5:

A 79-year-old right-handed woman presented with short-term memory loss for two years, with mild disorientation and irritability over the past 3 years. Her medical history included Paget's disease and hyperlipidemia. Her mother had "AD-like" dementia in her eighties. Cognitive assessments revealed difficulties with short-term memory, working memory, visuoperceptual tasks, phonemic fluency, and naming. Her initial MoCA score was 21/30. ASL-MR and FDG-PET suggested AD, particularly with decreased CBF and metabolism in the temporal lobes **(Figure 6, Online Supplemental File)**. Amyloid PET confirmed the AD diagnosis **(Online Supplemental File)**. Monitoring MRI scans before the 5th and 7th lecanemab infusions showed improvement in CBF and no ARIA **(Figure 6)**. Cognition was reported as stable by the family. Marked volume loss and mild white matter hyperintensity burden remained stable **(Online Supplemental File)**.

Case 6:

A 68-year-old man presented with progressive forgetfulness and personality changes over five years, including increased jealousy and irritability. His medical history included hypertension, hyperlipidemia and Type 2 diabetes. Cognitive assessment showed a MoCA score of 14/30, affected by poor vision and low educational attainment; his Clinical Dementia Rating (CDR) was 1.0. Family history included a mother with early-onset cognitive impairment and a brother with late-life paranoia.

ASL-MR and FDG-PET were concordant in suggesting AD **(Online Supplemental File)**; CSF biomarkers confirmed the diagnosis. The patient received initial treatment with donepezil and olanzapine with some improvement. Lecanemab therapy was then initiated. Monitoring MRI scans before the 5th and 7th infusions showed no ARIA and unchanged CBF **(Online Supplemental File)**; the patient's family felt his cognition had remained stable to slightly improved. Mild volume loss and minimal white matter hyperintensity burden remains stable **(Online Supplemental File)**.

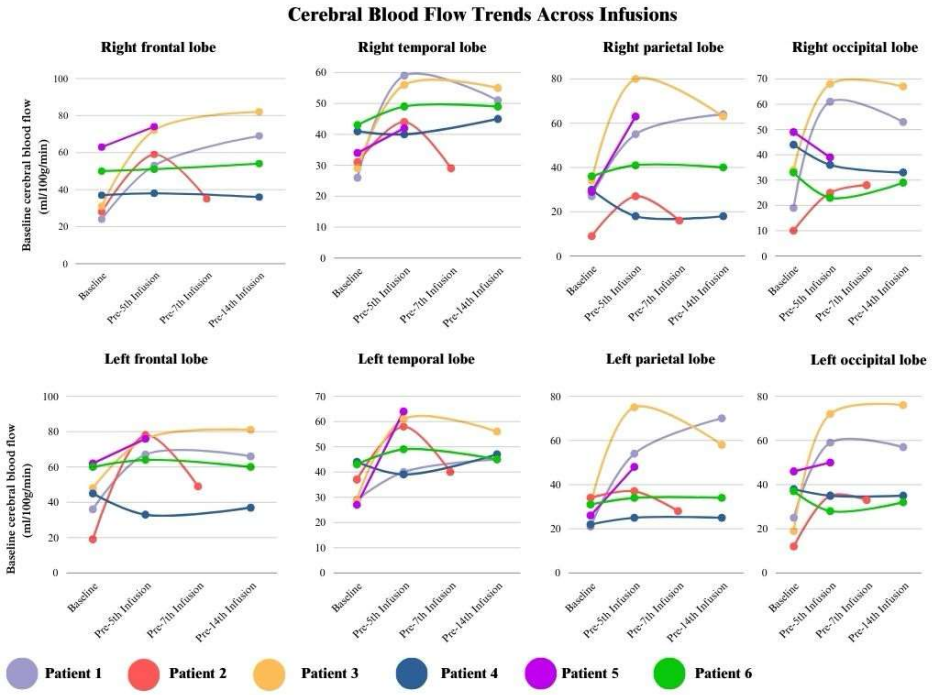

FIG 1. Line graphs showing trends in cerebral blood flow (CBF) values across time points. Data are shown for the six patients included in this case series, with measurements in the frontal, temporal, parietal, and occipital lobes, right or left.

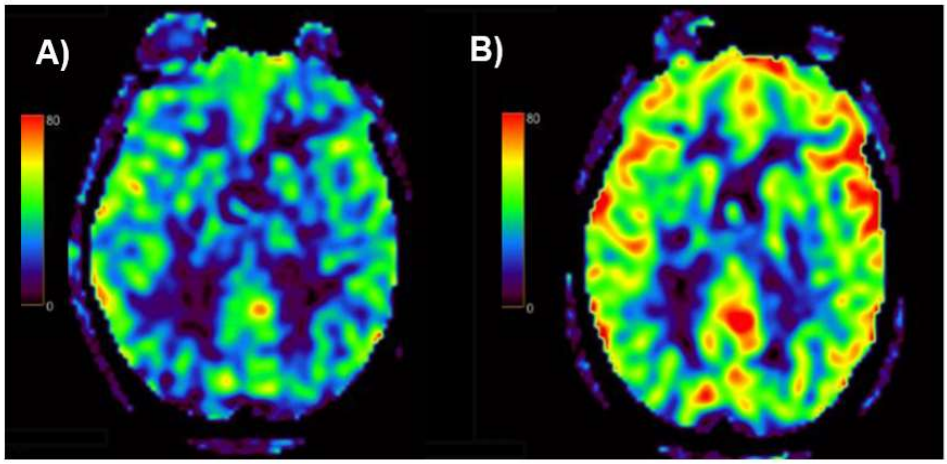

FIG 2. Patient 1 cerebral blood flow maps: (A) Baseline cerebral blood flow (CBF) map, before lecanemab treatment, demonstrating hypoperfusion, most prominently in the left frontal and bilateral parietal lobes. Post-treatment CBF map, obtained before the administration of the fifth dose of lecanemab (B), revealing marked overall increase in cerebral perfusion in all brain regions, which increases further on the CBF map before the 14th dose (C).

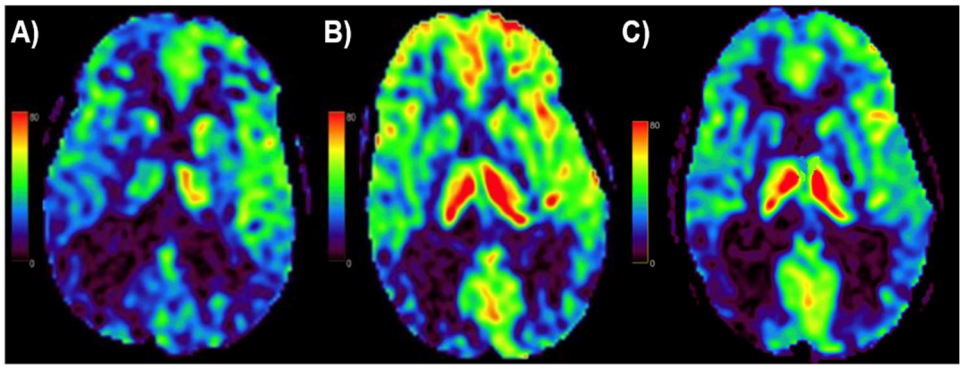

FIG 3. Patient 2 cerebral blood flow color map: A) CBF map showing hypoperfusion in the frontal, parietal, and occipital lobes, more pronounced on the right. B) CBF map after the fourth dose of lecanemab, demonstrating marked improvement in cerebral perfusion, especially in the bilateral frontal lobes. C) CBF map after the sixth dose of lecanemab, showing decreased overall perfusion compared to the post-fourth dose MRI, but still an improvement from baseline.

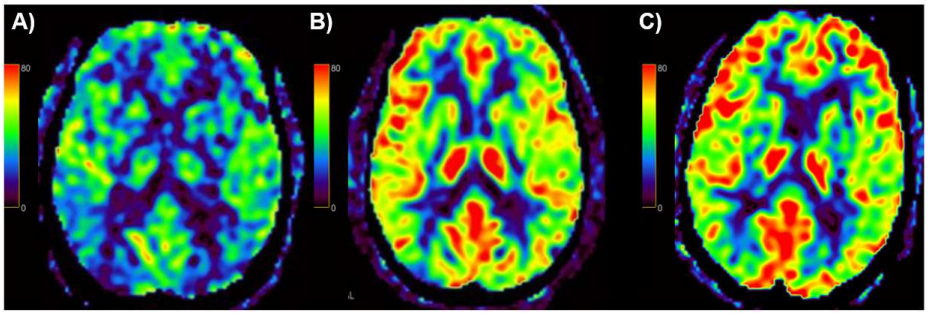

FIG 4. Patient 3 cerebral blood flow color map: A) Baseline CBF map showing reduced cerebral blood flow in the bilateral parietal lobes, with some involvement of the frontal lobes. B) CBF map after the 4th dose of lecanemab, with improvement in blood flow across the previously affected regions. C) CBF map after the 6th dose of lecanemab, showing further increased blood flow, compared to both the post-4th dose and baseline maps.

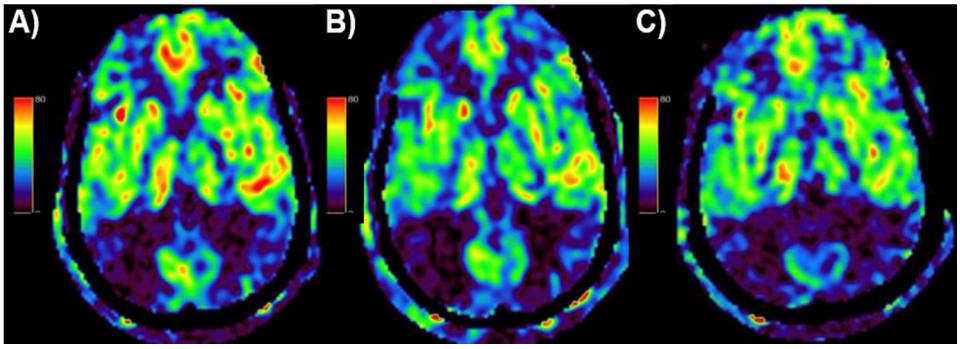

FIG 5. Patient 4 cerebral blood flow color map: A) Baseline CBF map showing hypoperfusion in the bilateral parietal lobes, as well as the right frontal lobe to a lesser extent. B) CBF map after the 4th dose of lecanemab, with no significant change in overall cerebral perfusion compared to baseline. C) CBF color map after the 13th dose of lecanemab, indicating no notable change in cerebral perfusion compared to the previous studies.

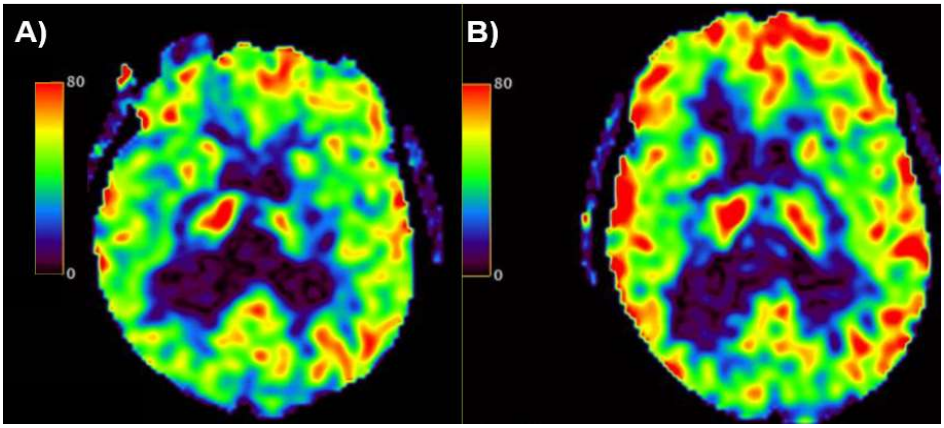

FIG 6. Patient 5 cerebral blood flow color map: A) Baseline CBF map showing cerebral blood flow to be within normal limits. B) After the 4th dose of lecanemab, the CBF color map showed generalized increase in cerebral perfusion.

DISCUSSION

The accumulation of amyloid-ß (Aß) extracellularly in brain parenchyma and along the walls of cerebral blood vessels is a well-described pathological characteristic of AD (9). Aß deposition in the walls and smooth muscle cells of cerebral arteries and arterioles, predominantly Aß-40, the short form of Aß, leads to decreased CBF (9,10). The cases presented in this series highlight how CBF changes on ASL-MR could reflect clearance of Aß on lecanemab therapy, thereby raising the possibility that ASL-MR could provide an early predictive biomarker of treatment response.

Similar to FDG PET, longitudinal decline in CBF is associated with cognitive decline (11,12,13), likely due to the tight coupling of blood flow, synaptic activity, and glucose metabolism (14). This series demonstrates that ASL-MR can provide valuable insights into the neurovascular effects of lecanemab within 2-3 months of therapy, with three patterns of CBF change demonstrated: continued improvement (Cases 1, 3, 5), immediate increase which reverts to baseline (Case 2), and no improvement (Cases 4 and 6). ASL-MR can thus potentially serve as a non-invasive, cost-effective method for tracking treatment progress before the slowing of cognitive decline can be detected (9).

In cases of increased CBF, antibody clearance by lecanemab may effectively clear vascular amyloid (15,16). Preclinical investigations have provided evidence that monoclonal antibody therapies can protect neurons from Aß-induced apoptosis, leading to neuronal viability and improved brain perfusion (17). CBF increases may also reflect increased synaptic activity after amyloid clearance and/or vascular changes, such as clearance of fibrinogen/amyloid clotting complexes (18), further leading to CSF clearance of toxic proteins and improved metabolic activity. Notably, Case 1's family reported cognitive improvement, and Case 3 demonstrated objective improvement on the MoCA.

In contrast, some patients did not exhibit significant changes in CBF despite lecanemab therapy. Cases 4 and 6, for instance, demonstrated persistently low CBF on serial ASL-MR studies. In Case 2, we observed improved CBF before the 5th dose, but this did not persist on the subsequent ASL-MR. An initial increase in cerebral blood flow may occur due to partial clearance of vascular amyloid. However, in advanced disease, the extent of amyloid clearance may be insufficient to mitigate disease progression, as other non-amyloid mechanisms may also cause a decline in CBF. These findings highlight varied hemodynamic changes, possibly providing a metric of underlying treatment efficacy. Notably Cases 2 and 4 had significant atrophy **(Online Supplemental File)**, which suggests that patients with more advanced disease may receive less benefit from therapy (1).

Our series highlights the potential for CBF to serve as a tool for monitoring the neurovascular effects of lecanemab. Unlike structural MRI, which primarily is used to monitor for ARIA-E and ARIA-H, ASL-MR provides both a qualitative and quantitative assessment of cerebral perfusion, which can reflect functional brain changes in response to treatment. The non-invasive nature and relatively low cost of ASL-MR allows it to be easily added to the MRI studies that are already mandated by the FDA during monitoring, further enhancing its suitability for routine clinical use, particularly when repeated measures are necessary. Our series is unique in that serial ASL-MR scans were performed on the same exact MRI scanner, mitigating technical reasons for CBF changes. However, validation of these results in larger cohorts is warranted, and future research can evaluate whether these early changes in CBF can predict true treatment efficacy, as demonstrated by amyloid clearance and slowing of cognitive decline.

This study has several limitations. As a case series, these findings may not be generalizable to the broader population of AD patients undergoing anti-amyloid therapies. Larger cohort studies are needed to validate these results and statistically evaluate the significance of CBF changes across serial ASL-MR. In addition, none of the patients presented had evidence of ARIA; future research will consider the potential effects of ARIA on CBF.

As noted in Table 1, several of our patients had vascular comorbidities, which were stable but could potentially influence CBF. We chose to not exclude patients with these vascular comorbidities because AD patients in real-world settings have high rates of these comorbidities and

are being treated with anti-amyloid therapies. For example, one study reported that almost half of their treated AD patients had hypertension, 24% had diabetes, and more than 70% had hypercholesterolemia (19). By including such patients in our clinical case series, we show that CBF maps could be informative in these populations as well.

Finally, this study relied on manual region of interest (ROI) analysis, which can be subject to user variability, potential bias, and partial volume effects. However, we chose this form of analysis for easy translation into clinical practice.

Notably, we observed an improvement in cognitive symptoms in cases 1, 3, and 6, although anti-amyloid therapies are primarily designed to slow disease progression rather than directly improve clinical symptoms. Further longitudinal clinical follow-up could provide insights into these cognitive improvements. Future work could also whether CBF changes reflect changes in cerebral metabolism on FDG-PET or glymphatic clearance using cerebrospinal fluid dynamics or diffusion metrics.

Table 1. Patient characteristics, including history of vascular risk factors.

Age	Confirmation of Alzheimer's pathology	APOE genotype	Baseline MoCA score	Hypertension	Dyslipidemia	Diabetes
77	Amyloid PET	E3/E3	23	Yes	Yes	No
59	CSF biomarkers	E3/E3	20	No	No	No
74	Amyloid PET	E3/E3	22	No	No	No
62	Amyloid PET	E3/E3	16 (MMSE 22)	No	Yes	No
79	Amyloid PET	E3/E3	21	No	Yes	No
68	CSF biomarkers	E4/E4	14 (CDR 1)	Yes	Yes	No

CONCLUSIONS:

This case series highlights a potential role for noncontrast ASL-MR to detect changes in CBF in AD patients receiving lecanemab therapy. The varied response to therapy shown in this case series, although not yet not well understood, suggests that CBF changes may provide an opportunity for personalized approaches to monitoring and treatment. ASL-MR offers a promising, non-invasive, and low-cost means to track these changes, which could enhance our understanding and management of AD in clinical practice. Further longitudinal studies are needed to determine whether early CBF improvements can predict better cognitive response to anti-amyloid and other upcoming forms of AD therapy.

REFERENCES

1. Cummings J, Apostolova L, Rabinovici GD, et al. Lecanemab: Appropriate Use Recommendations. J Prev Alzheimers Dis. 2023;10(3):362-377. doi: 10.14283/jpad.2023.30

2. FDA approves treatment for adults with Alzheimer's disease. U.S Food and drug administration. 2024 Jul 2; Available from: https://www.fda.gov/drugs/news-events-human-drugs/fda-approves-treatment-adults-alzheimers-disease

3. Soderberg L, Johannesson M, Nygren P, et al. Lecanemab, aducanumab, and gantenerumab - binding profiles to different forms of amyloid-beta might explain efficacy and side effects in clinical trials for Alzheimer's disease. Neurotherapeutics. 2023;20(1):195-206. doi: 10.1007/s13311-022-01308-6.

4. van Dyck C.H., Swanson C.J., Aisen P., et al. Lecanemab in early Alzheimer's disease. N. N Engl J Med. 2023;388(1):9-21. doi: 10.1056/NEJMoa2212948.

5. Lee K, Mahmud M, Marx D, et al. Clinical Arterial Spin-Labeling MR Imaging to Screen for Typical and Atypical Neurodegenerative Disease in the New Era of Alzheimer Treatment. AJNR Am J Neuroradiol. 2024;45(5):632-636. doi: 10.3174/ajnr.A8164.

6. Wierenga CE, Hays CC, Zlatar ZZ. Cerebral blood flow measured by arterial spin labeling MRI as a preclinical marker of Alzheimer's disease. J Alzheimers Dis. 2014;42 Suppl 4(Suppl 4):S411-9. doi: 10.3233/JAD-141467.

7. Wolk DA, Detre JA. Arterial spin labeling MRI: an emerging biomarker for Alzheimer's disease and other neurodegenerative conditions. Curr Opin Neurol. 2012;25(4):421-8. doi: 10.1097/WCO.0b013e328354ff0a.

8. Zago W, Schroeter S, Guido T, et al. Vascular alterations in PDAPP mice after anti-Aß immunotherapy: Implications for amyloid-related imaging abnormalities. Alzheimers Dement. 2013 Oct;9(5 Suppl):S105-15. doi: 10.1016/j.jalz.2012.11.010.

9. Uekawa K, Hattori Y, Ahn SJ, et al. Border-associated macrophages promote cerebral amyloid angiopathy and cognitive impairment through vascular oxidative stress. Mol Neurodegener. 2023;18(1):73. doi: 10.1186/s13024-023-00660-1.

10. Kakuda N, Miyasaka T, Iwasaki N, et al. Distinct deposition of amyloid-beta species in brains with Alzheimer's disease pathology visualized with MALDI imaging mass spectrometry. Acta Neuropathol Commun. 2017 Oct 16;5(1):73. doi: 10.1186/s40478-017-0477-x.

11. Raz L, Knoefel J, Bhaskar K. The neuropathology and cerebrovascular mechanisms of dementia. J Cereb Blood Flow Metab. 2016 Jan;36(1):172-86. doi: 10.1038/jcbfm.2015.164.

12. Hanaoka T, Kimura N, Aso Y, et al. Relationship between white matter lesions and regional cerebral blood flow changes during longitudinal follow up in Alzheimer's disease. Geriatr Gerontol Int. 2016; 16(7): 836-842. doi: 10.1111/ggi.12563.

13. Weijs RWJ, Shkredova DA, Brekelmans ACM, et al. Longitudinal changes in cerebral blood flow and their relation with cognitive decline in patients with dementia: Current knowledge and future directions. Alzheimers Dement. 2023;19(2):532-548. doi: 10.1002/alz.12666.

14. Chen Y, Wolk DA, Reddin JS, et al. Voxel-level comparison of arterial spin-labeled perfusion MRI and FDG-PET in Alzheimer disease. Neurology. 2011 Nov 29;77(22):1977-85. doi: 10.1212/WNL.0b013e31823a0ef7.

15. Zago W, Schroeter S, Guido T, et al. Vascular alterations in PDAPP mice after anti-Aß immunotherapy: Implications for amyloid-related imaging abnormalities. Alzheimers Dement. 2013 Oct;9(5 Suppl):S105-15. doi: 10.1016/j.jalz.2012.11.010.

16. Morgan D. Mechanisms of Abeta plaque clearance following passive A beta immunization. Neurodegener Dis. 2005;2(5):261-6. doi: 10.1159/000090366.

17. Qiao Y, Chi Y, Zhang Q, Ma Y. Safety and efficacy of lecanemab for Alzheimer's disease: a systematic review and meta-analysis of randomized clinical trials. Front Aging Neurosci. 2023;15:1169499. doi: 10.3389/fnagi.2023.

18. Chen ZL, Singh PK, Calvano M, et al. A possible mechanism for the enhanced toxicity of beta-amyloid protofibrils in Alzheimer's disease. Proc Natl Acad Sci U S A. 2023 Sep 5;120(36):e2309389120. doi: 10.1073/pnas.2309389120.

19. Shields LBE, Hust H, Cooley SD, et al. Initial Experience with Lecanemab and Lessons Learned in 71 patients in a Regional Medical Center. J Prev Alzheimers Dis 2024;11:1549-1562. doi: 10.14283/jpad.2024.159.

SUPPLEMENTAL FILES

Supplemental Figure 1: Representative regions-of-interest placed on cerebral blood flow maps.

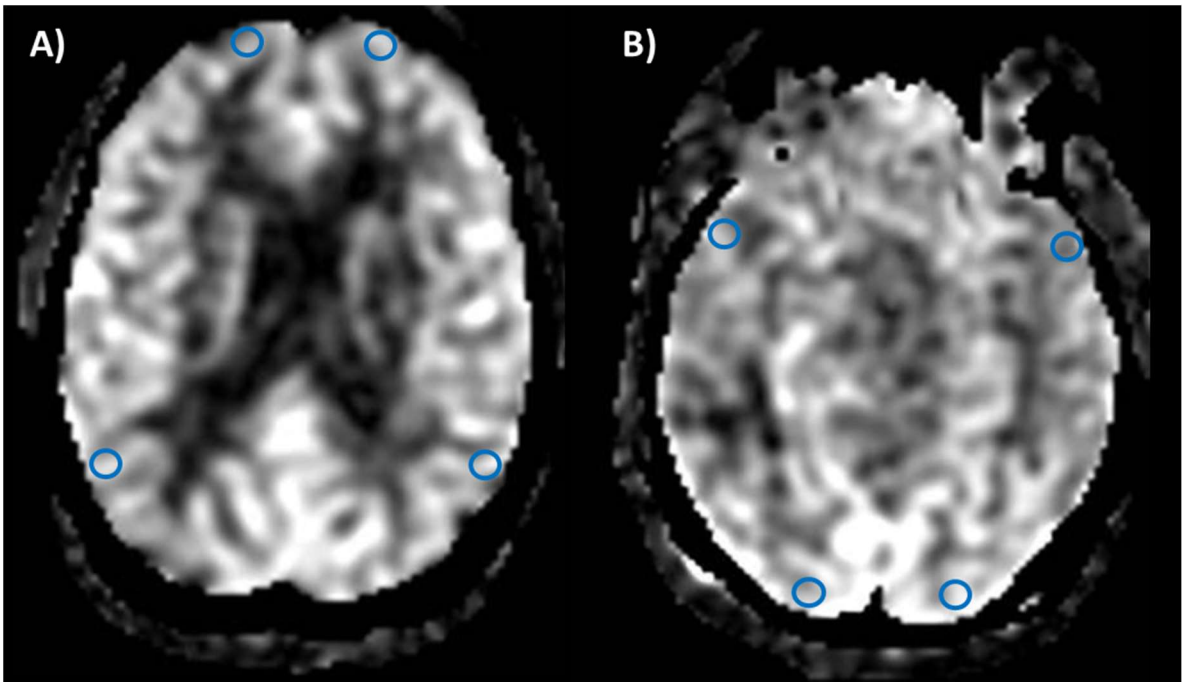

Representative regions-of-interest (circles) placed on cerebral blood flow maps, highlighting their localization within the **(A)** frontal and parietal cortices and **(B)** temporal and occipital cortices. These regions-of-interest were placed while blinded to all clinical information.

Supplemental Figure 2: Patient 1's FDG PET scan:

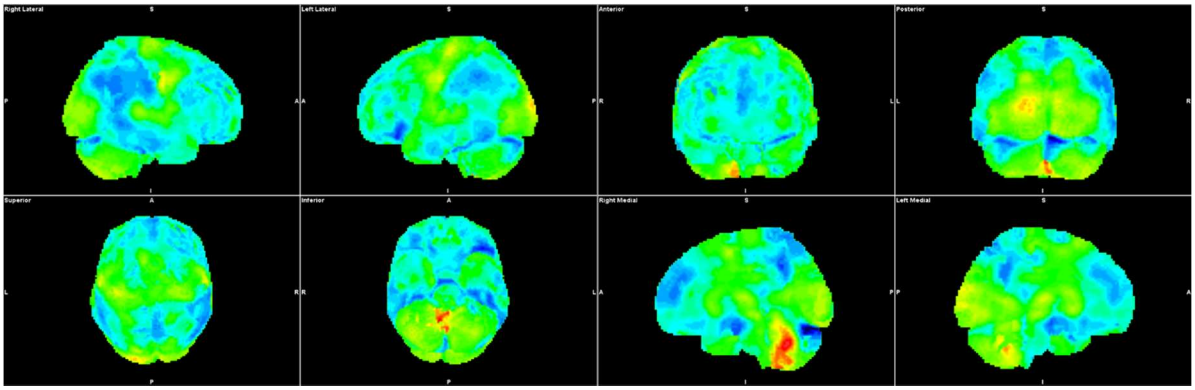

FDG PET 3D stereotactic surface projections showing decreased cerebral metabolism (blue) in the temporal and parietal lobes, as compared to a normative database, in a pattern suggestive of Alzheimer's disease. Frontal lobe involvement suggests more advanced disease.

Supplemental Figure 3: Patient 1's structural MRI and amyloid PET:

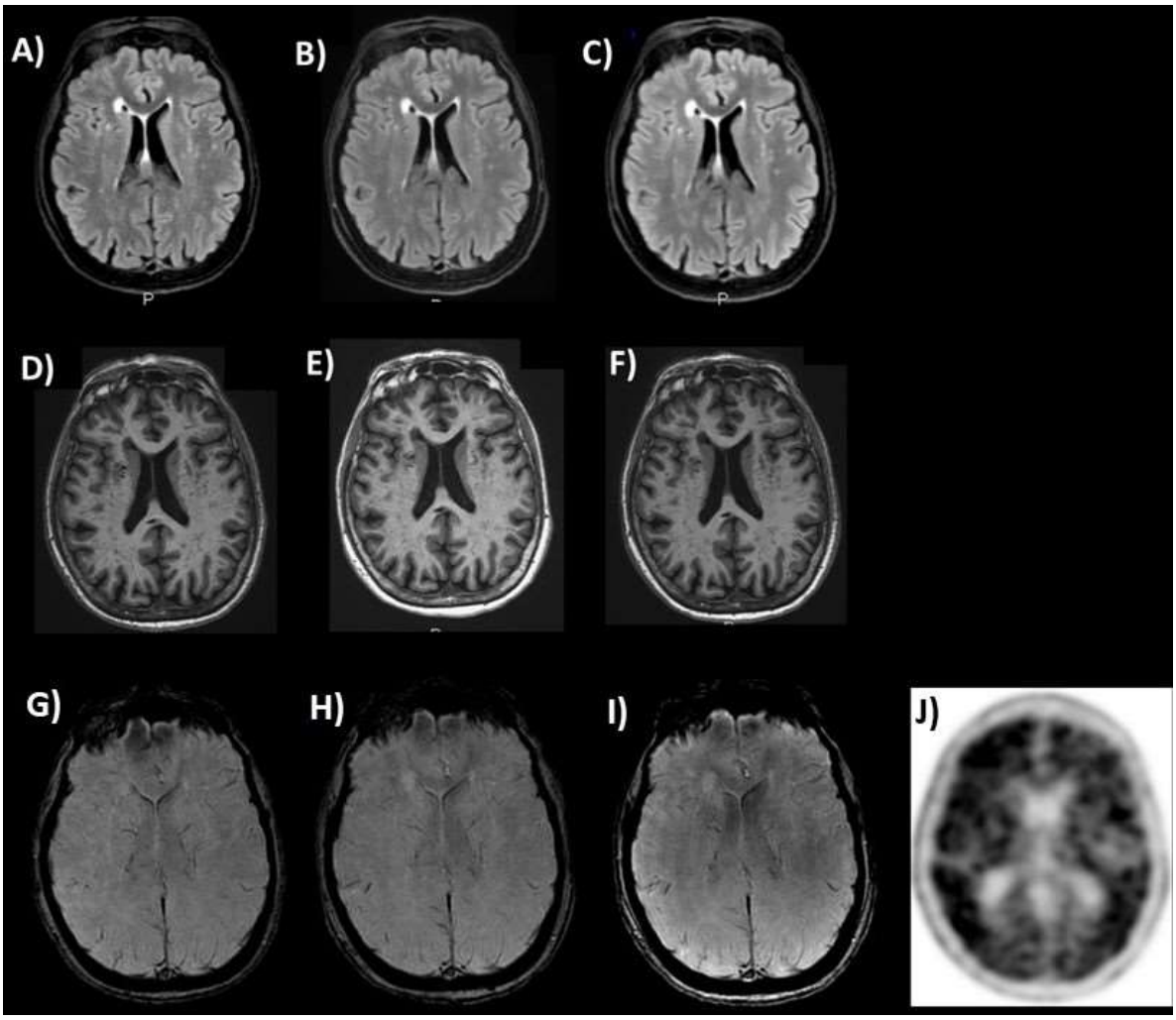

(A-C) 3D T2 FLAIR axial images showing a minimal burden of white matter hyperintensities at baseline and before the 5th and 14th infusions of lecanemab. There was no evidence of ARIA-E. **(D-F)** Corresponding 3D T1 MPRAGE axial images showing no significant difference in mild brain volume loss from baseline MRI on the pre-5th and pre-14th infusion MRI studies. **(G-I)** Corresponding SWI axial images showing no microhemorrhages or siderosis to suggest ARIA-H. **(J)** Positive amyloid PET scan confirms the diagnosis of Alzheimer's disease.

Supplemental Figure 4: Patient 2´s FDG PET

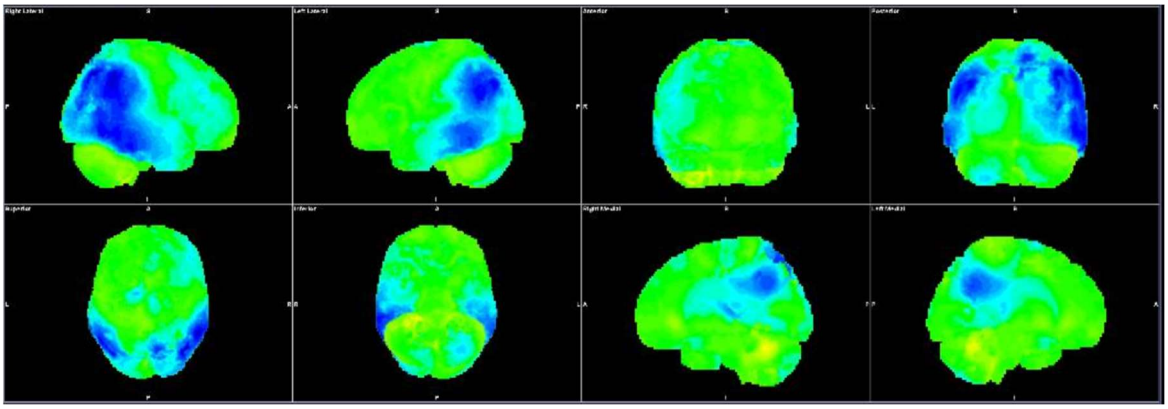

FDG PET 3D stereotactic surface projection images showing bilateral temporo-parietal hypometabolism (blue), including the precuneus bilaterally, as compared to a normative database, compatible with Alzheimer's disease.

Supplemental Figure 5: Patient 2´s structural MRI:

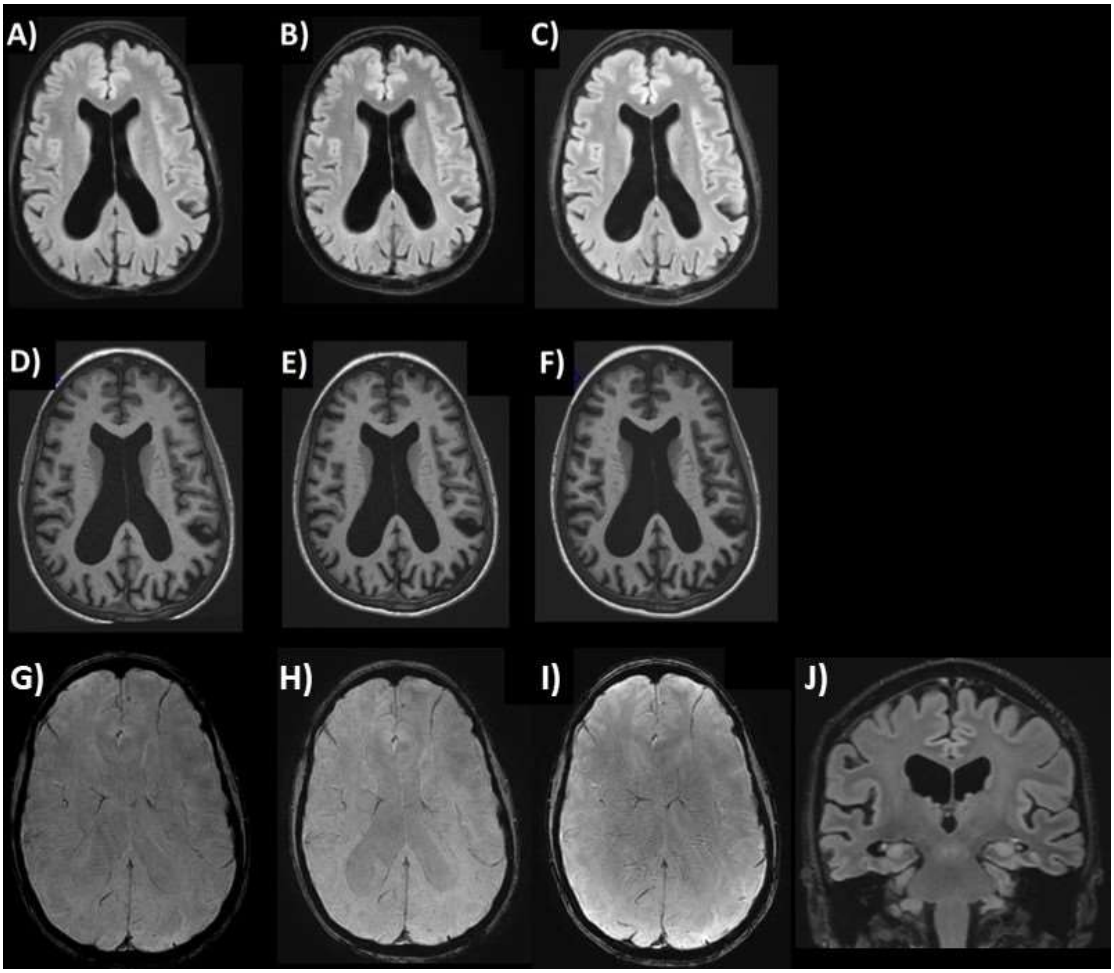

(A-C) 3D T2 FLAIR axial images showing a minimal burden of white matter hyperintensities at baseline and before the 5th and 7th infusions of

lecanemab. There was no evidence of ARIA-E. **(D-F)** Corresponding 3D T1 MPRAGE axial images showing no significant difference in marked brain volume loss from baseline MRI on the pre-5th and pre-7th infusion MRI studies. **(G-I)** Corresponding SWI axial images showing no microhemorrhages or siderosis to suggest ARIA-H. **(J)** Coronal T2 FLAIR showing no acute callosal angle, crowding at the vertex, or transependymal flow of CSF to suggest normal pressure hydrocephalus.

Supplemental Figure 6: Patient 3´s structural MRI and amyloid PET

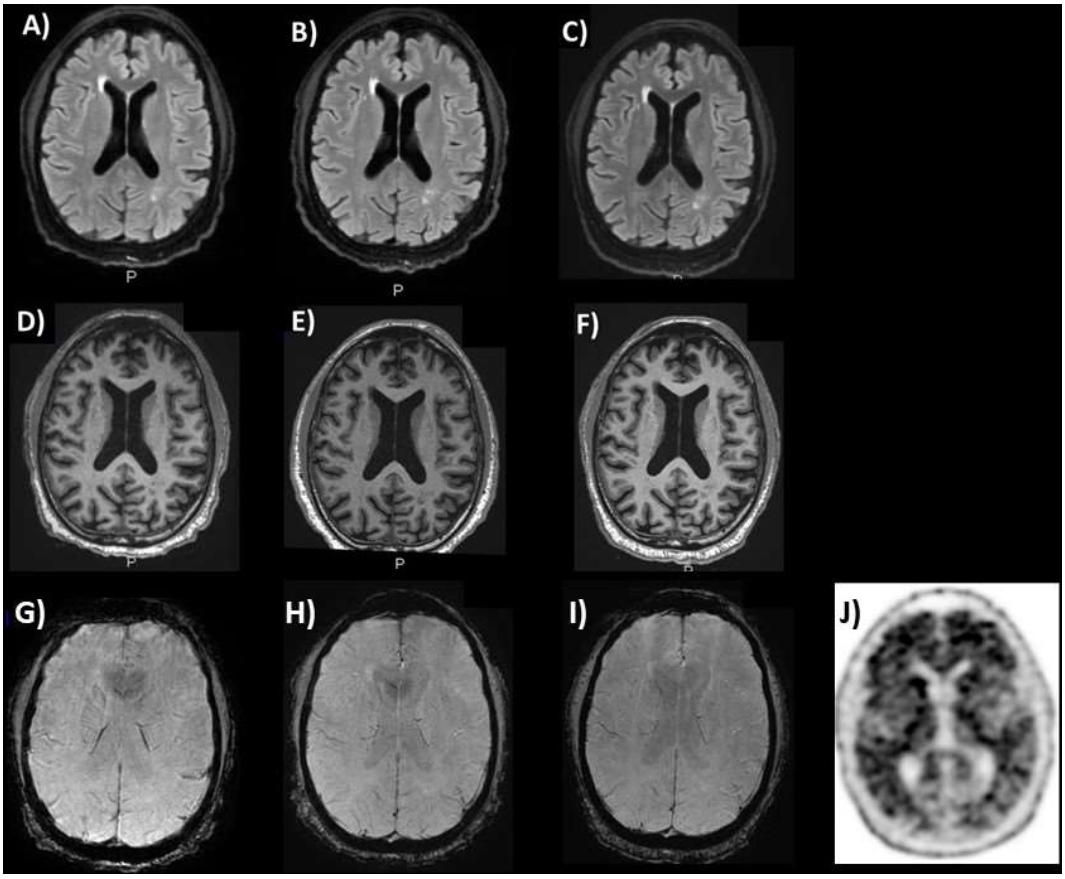

(A-C) 3D T2 FLAIR axial images showing a minimal burden of white matter hyperintensities at baseline and before the 5th and 14th infusions of lecanemab. There was no evidence of ARIA-E. **(D-F)** Corresponding 3D T1 MPRAGE axial images showing no significant difference in mild brain volume loss from baseline MRI on the pre-5th and pre-14th infusion MRI studies. **(G-I)** Corresponding SWI axial images showing no microhemorrhages or siderosis to suggest ARIA-H. **(J)** Positive amyloid PET scan confirms the diagnosis of Alzheimer's disease.

Supplemental Figure 7: Patient 4´s structural MRI and amyloid PET

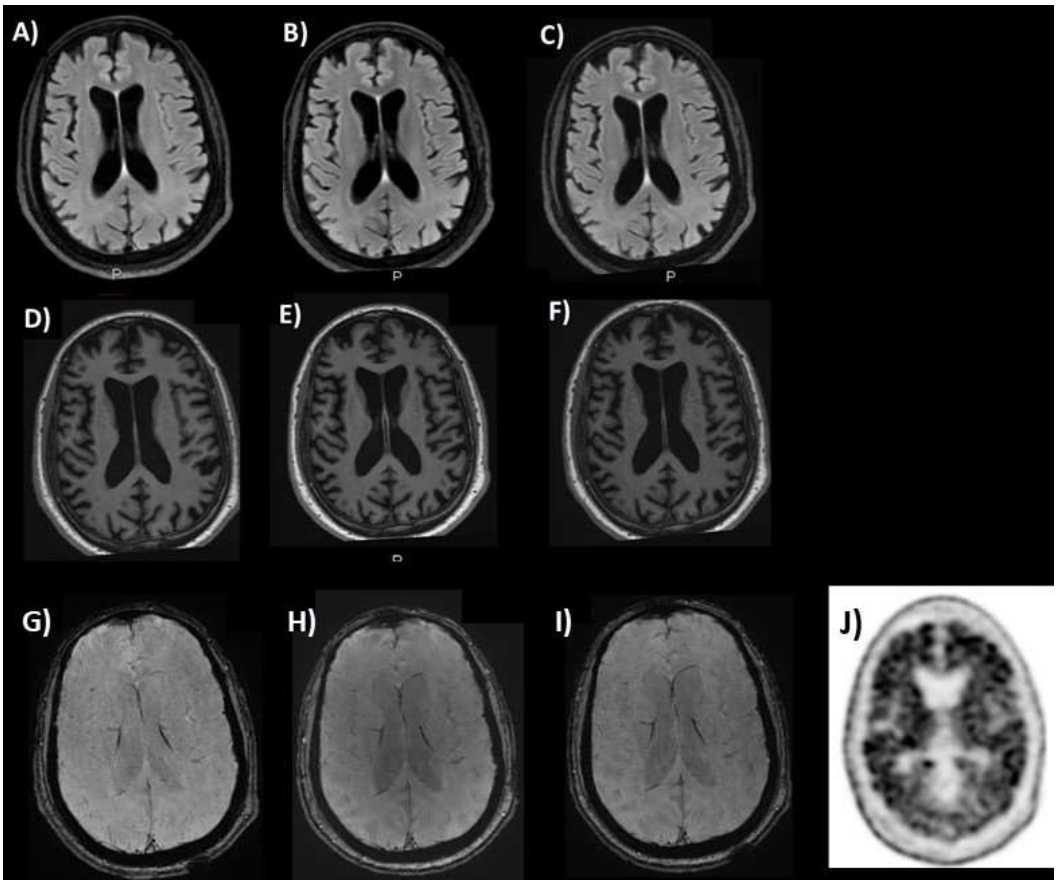

(A-C) Axial 3D T2 FLAIR images showing no white matter hyperintensities at baseline, before the 5th dose of lecanemab, and before the 14th dose. **(D-F)** Axial 3D T1 MPRAGE images show no significant difference in mild-moderate generalized volume loss across studies. **(G-I)** Corresponding SWI axial images showing no microhemorrhages or siderosis to suggest ARIA-H. **(J)** Positive amyloid PET confirming the diagnosis of AD.

Supplemental Figure 8: Patient 5´s FDG PET

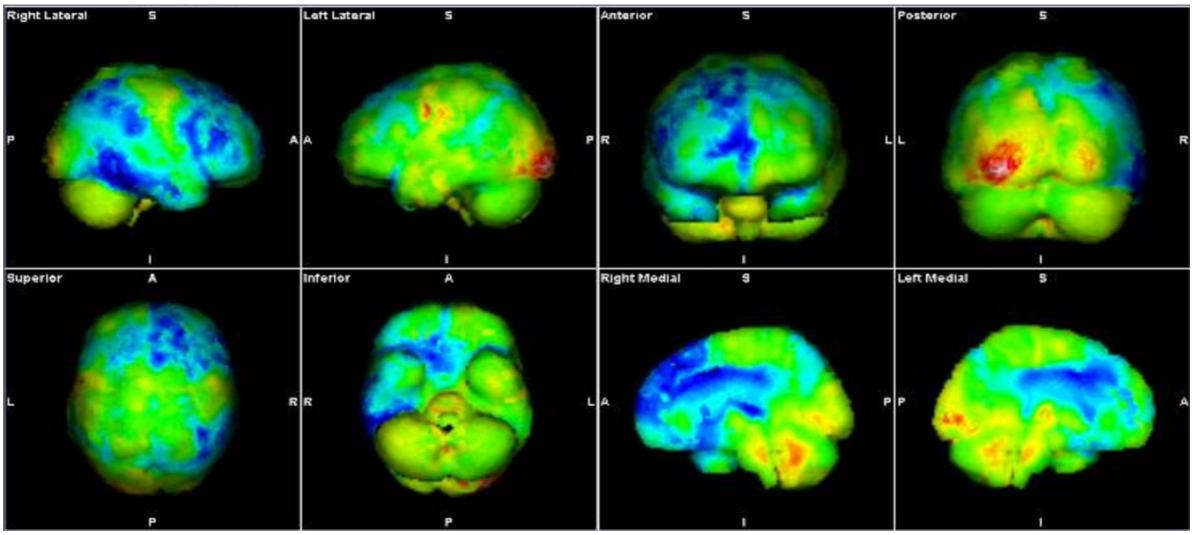

FDG PET 3D stereotactic surface projection images with predominantly right temporo-parietal hypometabolism, suggestive of AD, with some involvement of the right greater than left frontal lobes.

Supplemental Figure 9: Patient 5´s structural MRI and amyloid PET

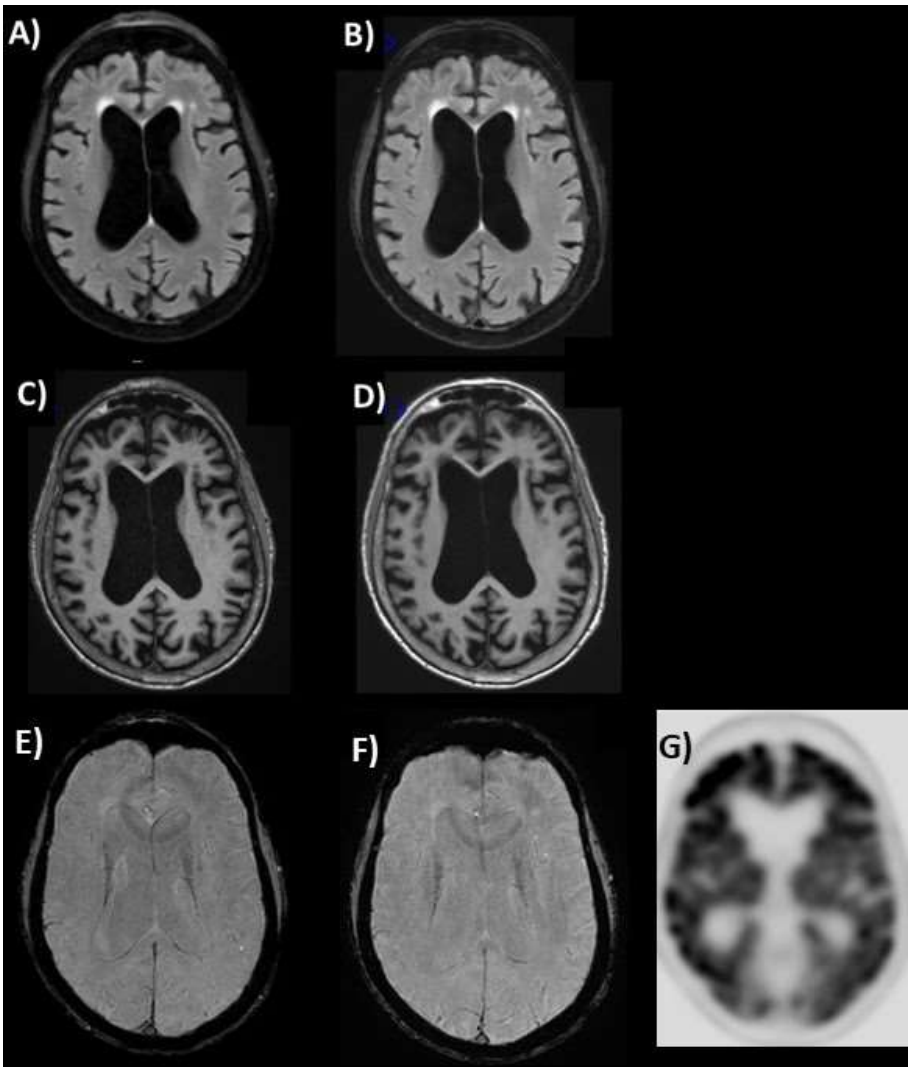

(A,B) Axial 3D T2 FLAIR images showing mild white matter hyperintensities at baseline and before the 5th dose of lecanemab. **(C,D)** No significant difference in marked volume loss between studies. **(E,F)** Corresponding SWI axial images showing no microhemorrhages or siderosis to suggest ARIA-H. **(G)** Positive amyloid PET confirming the diagnosis of AD.

Supplemental Figure 10: Patient 6's cerebral blood flow maps:

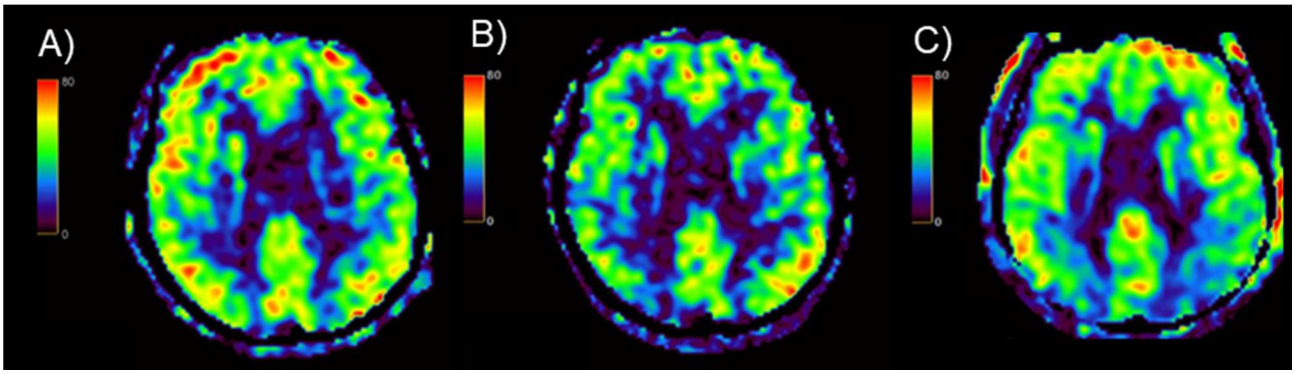

(A) Baseline CBF map showing overall normal cerebral blood flow. (**B)** CBF map before the 5th dose of lecanemab, showing slightly decreased perfusion overall, although within normal limits for age. **(C)** CBF map before the 7th dose of lecanemab, showing no significant change in perfusion from the prior.

Supplemental Figure 11: Patient 6´s structural MRI

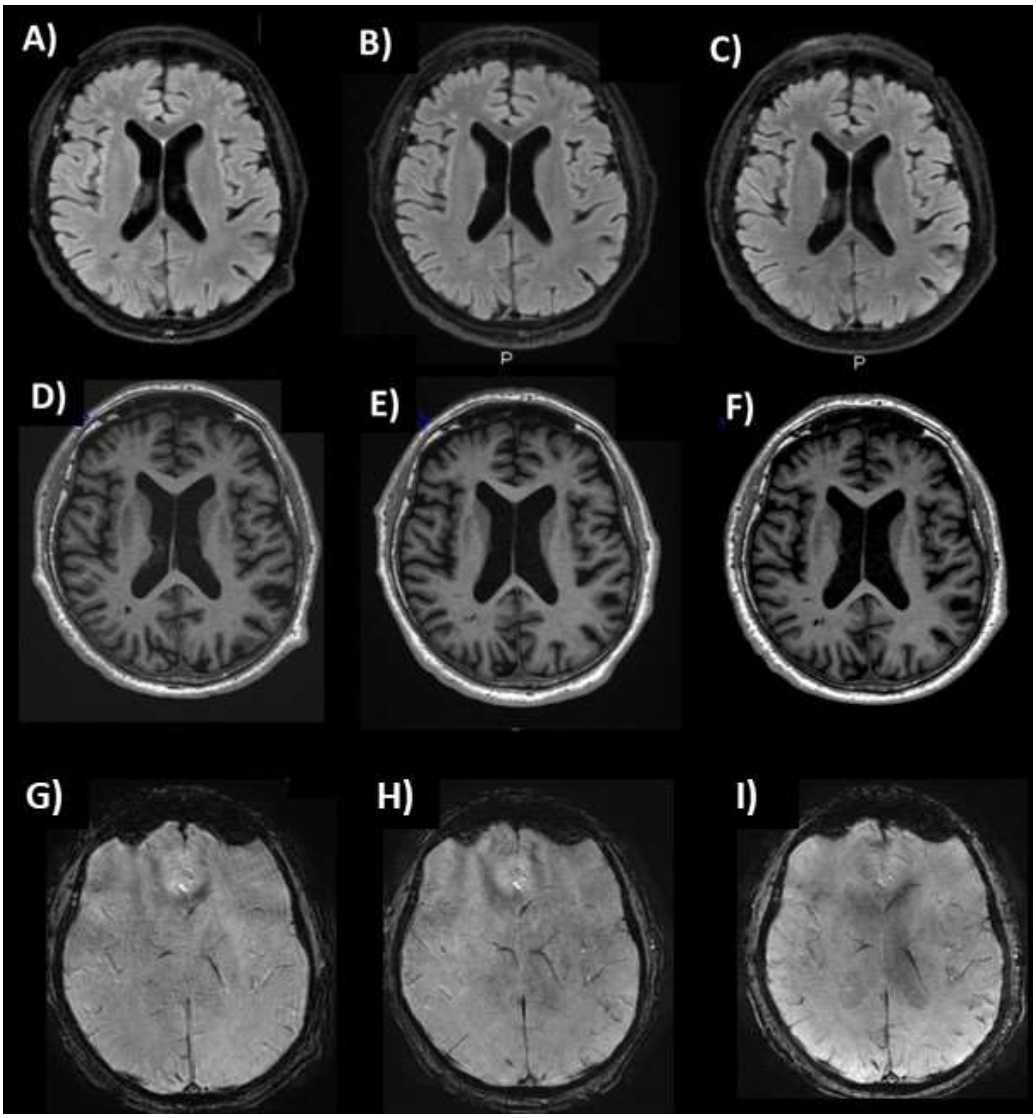

(A-C) Axial 3D T2 FLAIR images showing minimal white matter hyperintensities at baseline, before the 5th dose of lecanemab, and before the 7th dose of lecanemab . **(D-F)** Axial 3D T1 MPRAGE images indicating no significant difference in mild volume loss across the studies. **(G-I)** Corresponding SWI axial images showing no microhemorrhages or siderosis to suggest ARIA-H.

Supplemental Table 1: ASL-MR protocol parameters

IMAGING PARAMETERS		**SCAN TIMING**	
Imaging Mode	3D	**Number of Echoes**	1
Pulse Sequence	3D ASL	**Receiver Bandwidth**	62.50
Imaging Options	EDR, Fast, Spiral	**Post Label Delay**	2025.0
SCAN RANGE		**IMAGE ENHANCE**	
FOV	24.0	**Filter Choice**	None
Slice Thickness	4.0	**GATING/TRIGGER**	
Number of Slices	1	**Pause After Navigator Prescan**	0
ACQ TIMING		**FMRI**	
Freq	512	**PSD Trigger**	Internal
Phase	8	**View Order**	Bottom/Up
Freq DIR	R/L	**# of Repetitions REST**	0
NEX	3.00	**# of Repetitions ACTIVE**	0
Auto Shim	Auto	**SAT**	
Phase Correction	No	**Tag Type**	None
RF Drive Mode	Preset	**Fat/Water Saturation**	Fat
Excitation Mode	Selective	**TRICKS**	
USER CVS		**Pause On/Off**	On
User CV1	1.00	**Auto Subtract**	0
User CV2	1.00	**Auto SCIC**	Off
User CV Mask2	0		
MULTI-PHASE			
Separate Series	0		
Delay after Acquisition without AV	0		
Mask Phase	0		
Mask Pause	0		
Preserve	0		
DIFFUSION			
Recon All Images	On		
Multi b-values	1000.0		
Multi NEX Values	1.0		
# Synthetic b-values	1		
Synthetic b-value	1000.0		
CONTRAST			
Contrast Yes/No	No		

Supplemental Table 2. Qualitative and quantitative changes across ASL-MR studies. Qualitative assessments were performed using the rainbow color scale (range 0-80), with each follow-up scan compared to the baseline cerebral blood flow (CBF) map. For quantitative assessments, a circular region-of-interest (ROI) was placed on the cortical gray matter of each lobe to obtain the regional CBF. The ROI was placed in the same region on subsequent MRI studies.

Patient 1	Region	Baseline CBF (ml/100g/min)	Pre 5th infusion qualitative CBF	Pre 5th infusion CBF (ml/100g/min)	Pre 14th infusion qualitative CBF	Pre 14th infusion CBF (ml/100g/min)
cognition improved	Right frontal lobe	24	Increased	53	Increased	69
	Left frontal lobe	36	Increased	67	Increased	66
	Right temporal lobe	26	Increased	59	Increased	51
	Left temporal lobe	29	Increased	40	Increased	45
	Right parietal lobe	27	Increased	55	Increased	64
	Left parietal lobe	21	Increased	54	Increased	70
	Right occipital lobe	19	Increased	61	Increased	53
	Left occipital lobe	25	Increased	59	Increased	57
Patient 2	**Region**	**Baseline CBF (ml/100g/min)**	**Pre 5th infusion qualitative CBF**	**Pre 5th infusion CBF (ml/100g/min)**	**Pre 7th infusion qualitative CBF**	**Pre 7th infusion CBF (ml/100g/min)**
stable cognition	Right frontal lobe	28	Increased	59	Unchanged	35
	Left frontal lobe	19	Increased	78	Increased	49
	Right temporal lobe	31	Increased	44	Unchanged	29
	Left temporal lobe	37	Increased	58	Unchanged	40
	Right parietal lobe	9	Increased	27	Unchanged	16
	Left parietal lobe	34	Unchanged	37	Unchanged	28
	Right occipital lobe	10	Increased	25	Increased	28
	Left occipital lobe	12	Increased	35	Increased	33
Patient 3	**Region**	**Baseline CBF (ml/100g/min)**	**Pre 5th infusion qualitative CBF**	**Pre 5th infusion CBF (ml/100g/min)**	**Pre 14th infusion qualitative CBF**	**Pre 14th infusion CBF (ml/100g/min)**
cognition	Right frontal lobe	31	Increased	72	Increased	82

improved	Left frontal lobe	48	Increased	76	Increased	81
	Right temporal lobe	29	Increased	56	Increased	55
	Left temporal lobe	29	Increased	61	Increased	56
	Right parietal lobe	34	Increased	80	Increased	63
	Left parietal lobe	31	Increased	75	Increased	58
	Right occipital lobe	34	Increased	68	Increased	67
	Left occipital lobe	19	Increased	72	Increased	76
Patient 4	**Region**	**Baseline CBF (ml/100g/min)**	**Pre 5th infusion qualitative CBF**	**Pre 5th infusion CBF (ml/100g/min)**	**Pre 14th infusion qualitative CBF**	**Pre 14th infusion CBF (ml/100g/min)**
cognition worsened	Right frontal lobe	37	Unchanged	38	Unchanged	36
	Left frontal lobe	45	Unchanged	33	Unchanged	37
	Right temporal lobe	41	Unchanged	40	Unchanged	45
	Left temporal lobe	44	Unchanged	39	Unchanged	47
	Right parietal lobe	30	Unchanged	18	Unchanged	18
	Left parietal lobe	22	Unchanged	25	Unchanged	25
	Right occipital lobe	44	Decreased	36	Decreased	33
	Left occipital lobe	38	Decreased	35	Decreased	35

Patient 5	**Region**	**Baseline CBF (ml/100g/min)**	**Pre 5th infusion qualitative CBF**	**Pre 5th infusion CBF (ml/100g/min)**	
stable cognition	Right frontal lobe	63	Increased	74	
	Left frontal lobe	62	Increased	76	
	Right temporal lobe	34	Increased	42	
	Left temporal lobe	27	Increased	64	
	Right parietal lobe	29	Increased	63	
	Left parietal lobe	26	Increased	48	
	Right occipital lobe	49	Unchanged	39	
	Left occipital lobe	46	Unchanged	50	

Patient 6	Region	Baseline CBF (ml/100g/min)	Pre 5th infusion qualitative CBF	Pre 5th infusion CBF (ml/100g/min)	Pre 7th infusion qualitative CBF	Pre 7th infusion CBF (ml/100g/min)
stable to slightly improved cognition	Right frontal lobe	50	Unchanged	51	Unchanged	54
	Left frontal lobe	60	Unchanged	64	Unchanged	60
	Right temporal lobe	43	Unchanged	49	Unchanged	49
	Left temporal lobe	43	Unchanged	49	Unchanged	45
	Right parietal lobe	36	Unchanged	41	Unchanged	40
	Left parietal lobe	31	Unchanged	34	Unchanged	34
	Right occipital lobe	33	Decreased	23	Unchanged	29
	Left occipital lobe	37	Decreased	28	Unchanged	32

CBF = cerebral blood flow